Biochemical Engineering Journal 227 (2026) 110035

Contents lists available at ScienceDirect

Biochemical Engineering Journal

journal homepage: www.elsevier.com/locate/bej

Regular article

Effects of electrolyte composition and applied voltage on methane generation and microbial community shifts in the electromethanogenesis system

Lucky Caesar Direstiyani, Daisuke Inoue *, Michihiko Ike *

Division of Sustainable Energy and Environmental Engineering, Graduate School of Engineering, The University of Osaka, Suita, Osaka 565-0871, Japan

ARTICLE INFO

Keywords:
Electromethanogenesis
Electrode biofilm
Applied voltage
Electrolyte
Microbial community

ABSTRACT

An electromethanogenesis (EM) system was successfully established using non-acclimated anaerobic digestion sludge as the inoculum. This study aimed to evaluate the EM performance by varying the electrolyte composition and the applied voltage. Alterations in the microbial community associated with CH_4 generation and bio-electrochemchemical performance were also investigated. The findings indicated that the use of organic-rich electrolyte with a low applied voltage of 0.15 V showed a positive correlation with enhanced CH_4 generation up to 59 % and a CH_4 yield of 223.13 mmol day^{-1} m^{-2} which was ten times higher than the operation using the same electrolyte with an applied voltage of 0.35 V. Microbial community analysis revealed a shift of dominant methanogens from *Methanosaeta* to *Methanosarcina* and *Methanoculleus* at the cathodic biofilms when operated with organic-rich electrolyte at low voltage of 0.15 V. The presence of electroactive bacteria, such as *DMER64* and *JGI-0000079-D21*, and syntrophic bacteria, including *Desulfovibrio* and *Petrimonas*, suggested the development of syntrophic interactions that strengthen biofilm resilience and the overall performance of the EM system. The microbial interaction network also emphasized the significance of electrolyte composition and adequate applied voltage in shaping microbial biofilms for efficient CH_4 generation. The findings of this study accentuate the roles of sufficient electrolyte composition and low-voltage in enhancing the EM performance and corroborate the synergistic advantages of the EM system.

1. Introduction

While renewable energy production continues to increase globally, the reliable storage of surplus electricity to meet energy demand remains an essential challenge owing to the oscillation of renewable energy sources [1]. Power-to-gas technology offers a viable solution for transforming renewable energy into storable chemical energy, such as methane (CH_4) [2], and has attracted attention owing to its potential economic and environmental benefits when integrated into the energy sectors [3].

Electromethanogenesis (EM) is an emerging power-to-gas technology that can efficiently store surplus renewable electricity and transform CO_2 into CH_4 by engaging methanogenic biofilms [4–6]. Bio-electrochemical reactions in the combined EM-anaerobic digestion (AD) with a low-voltage supply can boost CH_4 production by enhancing microbial activity and promoting the degradation rate of organic matters, including volatile fatty acids (VFAs), toxic compounds, and less degradable matter [7–9]. The applied voltage affects the extracellular electron transfer, which encourages methanogens, in the EM [10]. Several studies have confirmed that the EM system can improve CH_4 content up to 84.81 % [11], 88.5 ± 1.4 % [12], and 98.9 ± 0.9 % [13], demonstrating biogas upgrade with EM.

To achieve efficient CH_4 production in an EM system, it is essential to construct and maintain an EM microbial community composed of diverse microbial populations associated with complex EM pathways [14]. Acclimatization has been commonly employed to establish EM microbial communities under different settings including inoculum sources, substrates, reactor configurations, electrode materials, and operating parameters [15–17]. However, due to the involvement of diverse microbial populations and their competitions in the EM systems [18], acclimatization generally requires a prolonged period of tens to hundreds of days [19–21], which is a significant issue to be addressed.

AD sludge is a potentially useful inoculum for the EM systems because it is composed of diverse synergistic anaerobic microorganisms

* Corresponding authors.
E-mail addresses: d.inoue@see.eng.osaka-u.ac.jp (D. Inoue), ike@see.eng.osaka-u.ac.jp (M. Ike).

https://doi.org/10.1016/j.bej.2025.110035
Received 2 September 2025; Received in revised form 19 November 2025; Accepted 28 November 2025
Available online 28 November 2025

that are involved in CH_4 production. It has been successfully used as an inoculum for the EM systems that produce CH_4 from different substrates, such as acetate and cattle manure [22], chicken manure [23], glucose [24], pre-treated waste activated sludge [25], and fishery processing wastewater [26]. However, these studies have employed specific reactor settings and operating variables. To date, no study has systematically evaluated the impact of key operating factors, particularly the influence of organic matter–dependent electrolyte, on the start-up and performance of EM systems inoculated with AD sludge, nor identified the critical parameters required to achieve rapid and stable EM performance.

Expanding upon current knowledge, this study aimed to 1) evaluate the effects of EM operating parameters in the start-up period with non-acclimatized AD sludge as the inoculum and 2) identify the core microorganisms in the EM system. Addressing the knowledge gap concerning the influence of organic matter–dependent electrolyte, this study investigated the effects of non-organic and organic-rich electrolytes under varying applied voltages. The findings provide novel insights to reveal the critical factors that govern the start-up and enhance the performance of EM system. The occurrence of core functioning microorganisms in the cathode biofilms for efficient CH_4 generation was analyzed using 16S rRNA amplicon sequencing.

2. Materials and methods

2.1. Inoculum and electrolyte composition

The AD sludge obtained from a mesophilic anaerobic digester in a municipal wastewater treatment plant in Japan was used as the inoculum. The AD sludge was centrifuged (4000 × *g*, 10 min) and washed twice with 0.9 % NaCl solution. The pH, total suspended solids (TSS) concentration and volatile suspended solids (VSS) concentration of the AD sludge were 7.10, 42 g L^{-1} and 33 g L^{-1}, respectively. The AD sludge was inoculated into the reactor at 4 g L^{-1} VSS at an inoculum-to-medium ratio of 1:5 (v/v).

Two different media were used as the electrolytes. The first medium was EM-electrolyte (EME) modified slightly from those of Alonso et al. [19] and Van Eerten-Jansen et al. [27], with the composition per liter of 0.87 g K_2HPO_4, 0.68 g KH_2PO_4, 0.04 g $CaCl_2{\cdot}2\ H_2O$, 0.1 g KCl, 0.453 g $MgCl_2{\cdot}6\ H_2O$, 0.25 g NH_4Cl, 0.5–2.25 g $KHCO_3$, and 10 mL each of vitamin and mineral solutions. Vitamin and mineral solutions were prepared as described by Marshall et al. [28]. The other medium was PY-electrolyte (PYE), with the composition per liter of 2.2 g yeast extract, 1.8 g peptone, and 2.25 g $KHCO_3$. During the replacement of the electrolyte at the start of each cycle, N_2 gas purging was performed for 30 min including 20 min (liquid phase) and 10 min (gas phase), to ensure anaerobic conditions. The pH of the medium ranged between 7.1 and 8.0 at the beginning of each cycle with no pH adjustment was made during the reactor operation.

2.2. Reactor configuration and operation

The schematic diagram of the reactor configuration is shown in Fig. 1. A single chamber-type reactor with an effective volume of 500 mL was set up. Two pieces and one piece of carbon felt (6 ×2 ×0.28 cm, F-350–1, Asahi Industry Co., Ltd., Japan) were used as working electrode and counter electrode, respectively, which were connected with titanium wire (inner diameter of 0.08 cm). The electrodes were pretreated by sequential immersion in 1 M nitric acid, 1 M acetone, and 1 M ethanol in sequence for 24 h each to avoid hydrophobicity and eliminate impurities, after which they were stored in distilled water until use. The reactor was placed inside an incubator maintained at 35 ± 1 °C. The reactor was continuously stirred using a magnetic stirrer (MLS-100C, ASONE, Japan) at 200 rpm to prevent mass transfer limitations. An ECStat-302 potentiostat (EC Frontier Co., Ltd., Japan) was used to provide the voltage to the reactor and record the cyclic voltammetry data. The gas generated from the reactor was collected using a 1 L aluminum gas bag (GL Sciences Inc, Japan).

The reactor was operated in the batch mode. The operating conditions are summarized in Table 1. The operation consisted of five stages

Table 1
Operations of experimental reactor.

Operation	Stage I	Stage II	Stage III	Stage IV	Stage V
Number of cycles	5 cycles	5 cycles	4 cycles	4 cycles	6 cycles
Duration (d)	36	30	24	28	30
Applied Voltage (V)	0.7	0.7	0.7	0.35	0.15
Electrolyte	EME	EME	EME	EME → PYE	PYE
$KHCO_3$ (g L^{-1})	0.5	1.5	2.25	2.25	2.25

Note: EME: EM-electrolyte; PYE: PY-electrolyte.

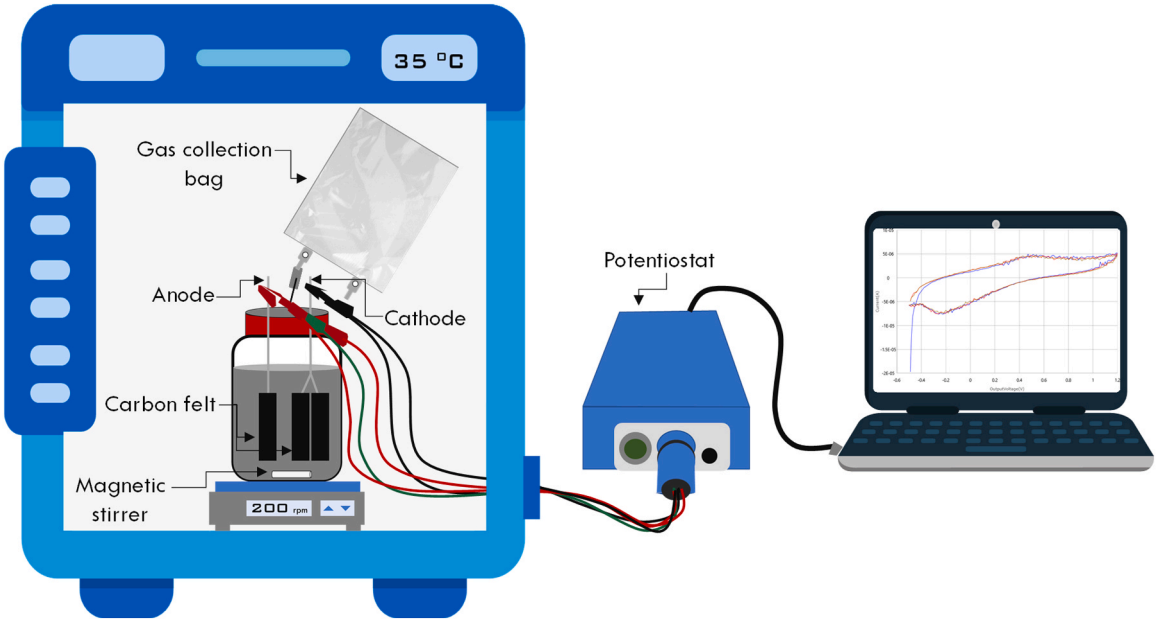

Fig. 1. Schematic of the reactor configuration.

with different electrolytes (EME and PYE) and applied voltages (0.15–0.7 V). Each stage consisted of 4–6 cycles with a duration of 3–10 days per cycle, depending on the current stability and CH_4 generation. Electrolyte replacement was performed when the current generation reached a steady-state level (fluctuations less than 5 % over 24 h) and no significant increase of CH_4 production, indicating the completion of a cycle. These indicators reflect stabilized electron transfer and methanogenic activity, marking the end of substrate turnover and justifying electrolyte replacement. The electrolyte was replaced at the beginning of each cycle to mitigate any limitations imposed by nutrient deficiencies or pH changes.

2.3. Analytical methods

The composition of the gas samples (H_2, CO_2, and CH_4) was measured at the end of each cycle using a GC-2010 Plus gas chromatography system (Shimadzu, Japan) equipped with a barrier discharge ionization detector and a MICROPACKED-ST capillary column (Shinwa Chemical Industries, Japan). The aqueous samples were centrifuged (4000 ×*g*, 10 min) and the supernatant was filtered through a 0.45 μm cellulose acetate filter (Advantec, Japan) prior to measurements of VFAs and soluble chemical oxygen demand (sCOD) concentrations. The concentration of VFAs was measured using a GC-2014 gas chromatography system (Shimadzu) with a flame ionization detector and a Stabilwax-DA capillary column (Restek, USA). The concentrations of acetate, propionate, butyrate, and valerate were calculated as COD (mg L^{-1}) with conversion coefficients of 1.07, 1.51, 1.82, and 2.04, respectively. The sCOD concentration was determined using a Merck COD Spectroquant test kit and a Move 100 colorimeter (Merck, Germany). The pH was measured at the beginning and end of each cycle using a TPX-999i pH meter (Toko Chemical Laboratories Co., Ltd., Japan). The TSS and VSS concentrations were measured using the gravimetric method following standard methods [29]. The energy conversion efficiency was calculated based on the density (0.09 kg m^{-3} and 0.72 kg m^{-3}) and the calorific value (142 kJ g^{-1} and 55.6 kJ g^{-1}) of the H_2 and CH_4 gases, respectively [30]. The energy recovery rate (kJ m^{-2} d^{-1}) was also calculated as the energy recovery per the total cathode surface area (m^2), which serves as the working electrode, and time (d). The H_2 conversion was estimated based on the stoichiometry of hydrogenotrophic methanogenesis ($CO_2 + 4\ H_2 \rightarrow CH_4 + 2\ H_4O$) and the hydrogen mass conservation equation (H_2 converted = Total H_2 produced – H_2 measured) to estimate the efficiency of H_2 utilization for CH_4 generation. Total H_2 production was estimated from the sum of measured H_2 accumulation in the headspace, gas bag, and the stoichiometric H_2 required for measured CH_4. Gas volumes were normalized to standard temperature and pressure and expressed in moles (22.414 L·mol^{-1}).

The bioelectrochemical performance at the initial and end of each cycle were analyzed based on cyclic voltammetry (CV) curve by using the potentiostat with the scan rate of 10 mV/s and voltage range of –0.5–1.2 V vs Ag $AgCl^{-1}$ (3 M KCl, + 0.208 V vs standard hydrogen electrode (SHE)) at 35 ± 1 °C. CV was also performed using a bare anode and a cathode filled with fresh medium to obtain an abiotic CV curve. Measurements of gas composition, pH, and sCOD and VFAs concentrations were performed in duplicate to confirm reproducibility, minimize analytical uncertainty, and verify data consistency. Meanwhile, CV analysis was conducted in triplicate to confirm electrochemical reproducibility.

Biofilm formation on the surface of the cathode was observed using scanning electron microscopy (SEM). The samples were pretreated using the procedures described by Kas and Yilmazel [31] and Isozumi et al. [32] with some modifications. Briefly, the electrodes were pretreated with 2 % paraformaldehyde (PFA) in 0.1 M cacodylate buffer at pH 7.4 for 1 h, after which they were completely covered with 2 % glutaraldehyde (GA) in 0.1 M cacodylate buffer at pH 7.4, and then refrigerated at 4 °C for approximately 8 h. After removing the PFA and GA solution, the samples were washed with 0.1 M cacodylate buffer for three times with 5-min intervals. The post fixation was performed with 1 % OsO_4 in 0.1 M cacodylate buffer (pH 7.4) for 2 h. Afterwards, a series of dehydrations was performed with 25 %, 50 %, 75 %, 95 % ethanol for 10 min each. The samples were then incubated twice with 100 % t-butanol for 15 min at room temperature and coated with a 4–5 nm palladium coating. SEM was performed using a JCM-6000Plus NeoScop microscope (JEOL, Tokyo, Japan).

2.4. Microbial community analysis

Microbial DNA was extracted from 0.5 mL samples using the FastDNA Spin Kit for Soil (MP Biomedicals, USA). The PCR primers 515 F and 806 R were used to amplify the V4 region of the 16S rRNA genes [33,34]. Amplicon libraries were subjected to Illumina NextSeq 1000 sequencing (Illumina, USA) at the Bioengineering Lab. Co. Ltd., Kanagawa, Japan. The sequencing reads were quality filtered and exclude chimeric and noise sequences were checked by using DADA2 plugin in QIIME2 (ver 2024.2). The representative sequences were grouped into amplicon sequencing variants (ASVs). The taxonomic classification was assigned based on the SILVA database (ver 138.1) with 99 % identity. Sequencing depth was evaluated using rarefaction curves of ASVs for each sample plotted against sequence reads and Good's coverage, both were performed using R (ver 4.4.1, R Foundation, USA) with "vegan" package, to ensure that microbial diversity was sufficiently captured in all samples. In addition, the Kyoto Encyclopedia of Genes and Genomes (KEGG)-based metabolic pathway analysis using PICRUSt2 method [35] through QIIME2 was performed to predict the relative abundance of key enzymes involved in the EM system and potential metabolic mechanisms underlying the EM process. Raw sequencing data were deposited in the DNA Data Bank of Japan (DDBJ) with links to the BioProject accession number PRJDB35931.

2.5. Statistical analysis

All the statistical analyses were performed using R. The Pearson correlation matrix for each defined parameter were generated using the "corr_coef" function of the "metan" package. In the Pearson correlation analysis, the electrolyte type was coded as 1 and 2 for EME and PYE, respectively. The ASVs with Pearson correlation coefficient $r \geq 0.5$ and $p < 0.05$ (confidence interval of 95 %) were considered statistically significant and used for microbial co-occurrence network analysis. The networks were visualized using Gephi 0.10.1 [36]. The Fruchterman-Reingold layout was applied to optimize, sort, and detect distinct modules of microbial populations within each network. Redundancy analysis (RDA) was performed to investigate the relationship between CH_4 generation and microbial communities.

3. Results and discussion

3.1. EM reactor performance

The reactor started operating with EME as electrolyte at stage I with a stepwise increasing of inorganic carbon source ($KHCO_3$) concentration from 0.5 to 2.25 g L^{-1} and an applied voltage of 0.7 V (Table 1). Upon five consecutive cycles of stage I, the production of H_2 reached 98.13 %, accompanied by a low CO_2 (1.9 %) and no CH_4 generation. The pH performance demonstrated that increasing $KHCO_3$ from 0.5 to 2.25 g L^{-1} notably affected the initial pH in each cycle (Fig. S1). Specifically, the initial pH ranged from 7.10 to 7.30 at 0.5 g L^{-1} of $KHCO_3$, slightly raised to 7.25–7.42 when $KHCO_3$ concentration was increased to 1.5 g L^{-1}, and further increased to 7.49–8.04 at 2.25 g L^{-1} of $KHCO_3$. This was likely due to the enhanced buffering capacity by the increment of $KHCO_3$ concentration, which in turn stabilized the pH and mitigated acidification caused by VFAs accumulation and thus might support stable microbial metabolic activities including promote EM performance.

The operation was continued with EME until stage III with the gas generated in each cycle fluctuated from 48.73 to 290.47 mL that consisted exclusively of H_2 up to 97.4 %, with no CH_4 (Fig. 2a). VFAs accumulation was generally low, except for temporal high accumulation at the end of stages II and III, reaching total VFAs concentrations of 2029 and 3125 mg L^{-1}, respectively (Fig. 2b). This suggests the vigorous occurrence of water electrolysis along with the consequent abiotic and biotic H_2 generation in the reactor.

At cycle 1 of stage IV, the applied voltage was decreased to 0.35 V without changing the electrolyte type. This resulted in a further increase in H_2 gas content to 99.1 % with no CH_4 production. Generation of H_2 under biological conditions theoretically requires an applied potential of 0.14 V, however practical operation requires applied voltage above this threshold owing to cathodic overpotentials [37]. Along with high H_2 generation, the pH fluctuated between 7.2 and 8.5, which gradually increased during stage IV- cycle 1. An increase in the pH above 8.0 allows to generate more energy for electrogenic H_2 conversion, providing electrogens with a greater energy advantage over methanogens [38]. The dominance of water electrolysis and abiotic-biotic H_2 generation at the cathode can slow down or inhibit methanogens when CO_2 is not readily available. This is due to the shift in the equilibrium of the reaction towards the reactants, making it more difficult for methanogens to produce CH_4. Carrillo-Peña et al. [20] demonstrated that the absence of carbon source led to high H_2 generation up to 98 %. Similarly, limited

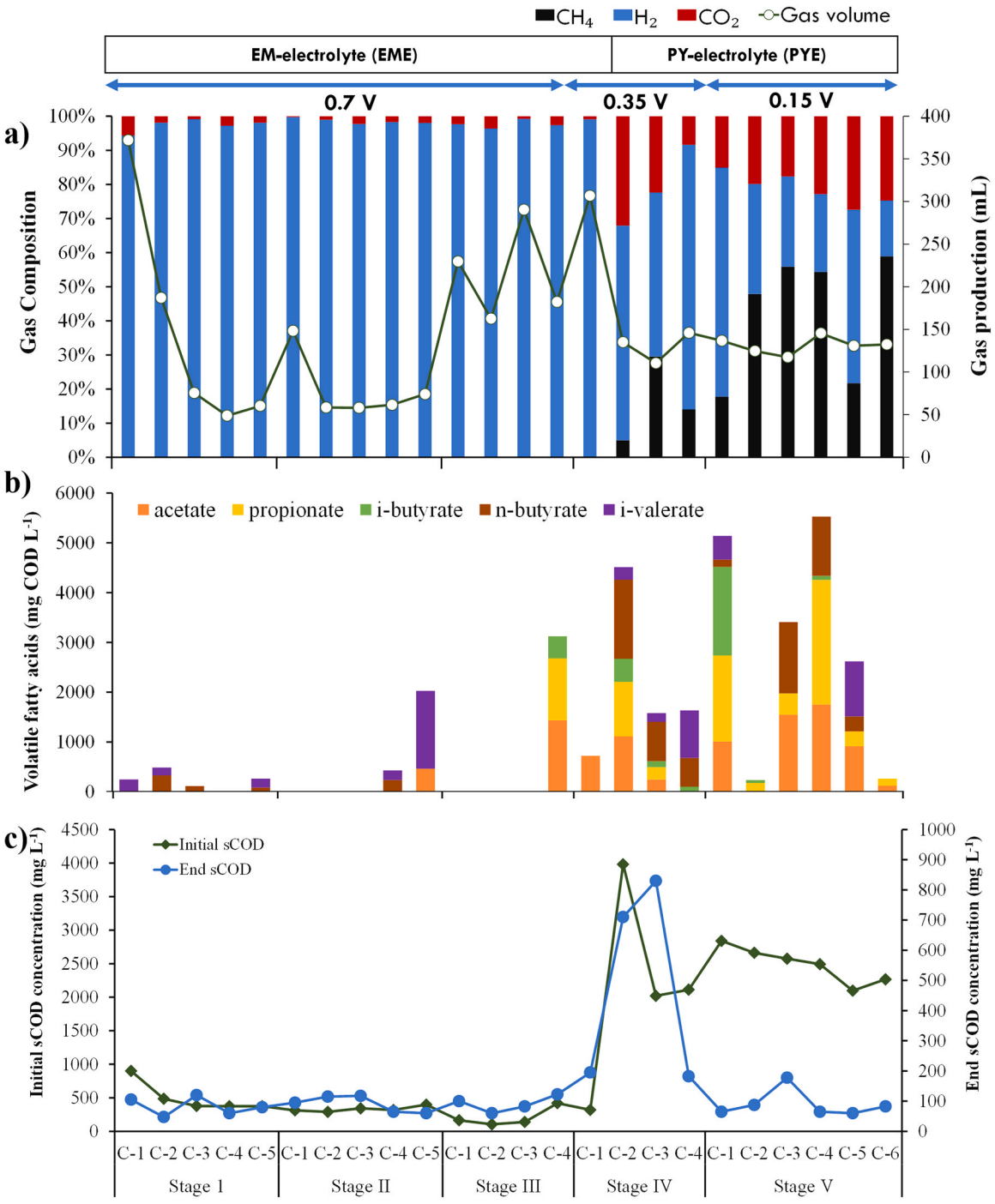

Fig. 2. Performance of experimental reactor in repeated cycles with different electrolyte compositions and applied voltages: a) gas content composition and gas production, b) VFAs performance at the end of each cycle, and c) sCOD concentration.

CO_2-feeding condition resulted in the dominance of H_2 production reaching up to 96 % [39].

Reactor performance with EME was also deteriorates owing to no organic matter addition, leading to the famine condition over a prolonged time. This is consistent with the findings of Hao et al. [40] and Wang et al. [41], who observed a declined performance associated with a decrease in active bacteria (biomass decay) and a reduction in specialized activity through starvation. The results obtained without the external addition of organic substrates contradicted with those in previous studies [8,19], both of which utilized a similar electrolyte composition but with external organic substrates and succeeded in CH_4 generation. This suggests that organic substrates are essential for CH_4 generation in EM system.

To confirm the hypothesis, the electrolyte was changed to PYE in stage IV-cycle 2, while maintaining the addition of 2.25 mg L^{-1} $KHCO_3$ and the applied voltage at 0.35 V. Resultantly, CH_4 was generated at 37.3 % (23.2 mL), with a decline in H_2 gas to 39.7 % (106.7 mL) at the end of stage IV (Fig. 2a). Meanwhile, VFAs accumulation reached 4510 mg L^{-1} at cycle 2 and thereafter alleviated to 1636 mg L^{-1} at cycle 4, with an enhancement of sCOD removal of 1930 L^{-1} (91.4 %) (Fig. 2b-c). In stage V, the applied voltage was lowered to 0.15 V. Consequently, CH_4 generation increased to 58.9 % (71.9 mL) in stage V-cycle 6. The sCOD removal and pH were maintained at approximately 96 % (2185 mg L^{-1}) and 7.6–7.8, respectively. At the end of stage V, the accumulation of VFAs was decreased to 262 mg L^{-1}, with the major composition of acetate (120.4 mg L^{-1}) and propionate (141.5 mg L^{-1}).

The decrease in VFAs accumulation along with enhanced sCOD removal indicates beneficial effects on acetogenesis. The decreased concentration of VFAs also aligned with the results of microbial analysis, which revealed an increased abundance of acetogens (ACE) and propionate-oxidizing bacteria (PRO-OB), which will be discussed below. VFAs in the EM system are first degraded into intermediate compounds such as hydrogen, formate, and acetate before generation of CH_4. The presence of electroactive bacteria (EAB) facilitate electron transfer during this process, enhancing the syntrophic oxidation of VFAs to H_2 and CO_2, which are then utilized by methanogens to produce CH_4. In contrast, under the EME condition without organic carbon, the available VFA concentration was extremely low, suggesting minimal substrate availability for syntrophic oxidation and subsequent methanogenesis. This resulted in reduced electron supply for CO_2 reduction to CH_4. Therefore, the observed CH_4 generation under the PYE–0.15 V condition can also be attributed to the efficient conversion of VFAs into intermediate electron donors, which in turn drove hydrogenotrophic and direct interspecies electron transfer (DIET) pathways during EM process. Thus, the utilization of PYE successfully encouraged CH_4 generation.

The PYE is composed of sufficient amounts of easily degradable organic matters. The high degradability of organic substrates in the EM systems is linked to the high activity of EAB, consequently electrons can be efficiently transferred to the cathode with high current density [42]. The yeast extract in PYE is rich in organic compounds and includes flavins and quinones that may function as electron shuttles to potentially facilitate extracellular electron transfer in electroactive microbial communities [43,44]. In contrast, EME lacking organic carbon failed to generate CH_4 and resulted in low electrochemical performance. These findings indicate that enhanced CH_4 generation is primarily driven by the use of PYE, which provides essential substrates, electrons, and protons for microbial metabolisms. Additionally, redox-active compounds such as flavins and quinones in PYE may facilitate extracellular electron transfer, further supporting enhanced CH_4 generation.

Meanwhile, the increase of CH_4 productivity by applying a lower applied voltage in EM systems was demonstrated in Liu et al. [10] and Villano et al. [45]. Our results also found that the enhanced substrate hydrolysis and CH_4 productivity occurred with the applied voltage of 0.15 V compared to 0.35 V. Therefore, the combination of PYE and reduced applied voltage proved effective for obtaining an enhanced EM performance. However, as the PYE was assessed under 0.35 V and 0.15 V, its role in promoting EM performance requires further studies across varied applied voltage to clarify its effect on CH_4 generation.

Moreover, the H_2 conversion analysis indicated that the efficiencies of H_2 conversion were remarkably high under the PYE–0.15 V condition, with more than 80 % in most cycles and the maximum value of 94.4 % in cycle 6 (Table S1). These findings demonstrated that the majority of the generated H_2 was effectively utilized for CH_4 production rather than accumulated in the headspace or lost. This indicates an efficient coupling between bioelectrochemical H_2 generation and methanogenic H_2 consumption. High H_2 conversion efficiency under low-voltage PYE conditions suggests the dominance of syntrophic and hydrogenotrophic methanogenesis pathways, where bioelectrochemically produced H_2 serves as an immediate substrate for methanogens. The synergistic effect of organic-rich electrolyte (PYE) and low voltage (0.15 V) likely enhanced electron transfer and maintained a stable redox environment that favored efficient H_2 utilization and CH_4 formation.

Based on the results of H_2 and CH_4 generation, the energy recovery under different operating conditions was estimated (Table 2). The H_2 energy recovery is noticeably lower than that of CH_4 due to H_2 offers less energy per unit volume [46]. Consequently, the highest total energy recovery (215 kJ/m^2/d) was obtained using PYE at stage V with an applied voltage of 0.15 V, proving the positive effect of combining organic electrolyte and a lower applied voltage.

3.2. Bioelectrochemical performance and biofilm formation

The CV analysis revealed that the redox peaks did not appear during stage I to stage IV-cycle 1, consistent with the dominant generation of H_2 gas, as found in the abiotic control using a bare electrode and fresh medium (Fig. 3a). These results corroborated the exclusive occurrence of water electrolysis during this period. No observable redox peaks indicated a lack of electron shuttles linked to the biocathodes [28]. Meanwhile, after the electrolyte was changed to PYE and notable CH_4 generation occurred (stage IV-cycle 3 onwards), the CV graph exhibited a clear sigmoidal shape with redox peaks (Fig. 3b). The CV profile under the PYE conditions displayed clear oxidation (~ +0.52 V) and reduction (~0.42 V and −0.36 V) peaks with peak current up to 0.038 mA, indicating enhanced electrochemical activity relative to the EME condition (0.003 mA). These observations confirmed the enhancement of redox-active biofilm and electron transfer capacity by the use of PYE.

The sigmoidal current-generation profile and plateau catalytic current demonstrated microbial catalysis of direct electron transfer from the cathode to the microorganisms [28]. Direct electron transfer reflected by a sigmoidal CV curve has been observed in exoelectrogens, such as *Geobacter* [47]. The voltammogram width also increased substantially compared to the earlier stages with dominant H_2 generation and abiotic electrode, indicating an enhanced electrical capacitance that was linked to the development of electroactive biofilms. Higher current performance that was also obtained at the end of operation suggesting

Table 2
Total energy recovery with different electrolyte composition and applied voltage.

Operation	H_2 production		CH_4 production		Total energy recovery (kJ /m^2/d)
	H_2 yield (mmol/m^2/d)	Energy recovery (kJ /m^2/d)	CH_4 yield (mmol/m^2/d)	Energy recovery (kJ /m^2/d)	
EME - 0.7 V	270.95	77.56	0.00	0.00	77.56
EME - 0.35 V	471.16	134.88	0.00	0.00	134.88
PYE - 0.35 V	99.25	28.41	21.59	19.36	47.77
PYE - 0.15 V	52.96	15.16	223.13	200.08	215.24

Note: EME: EM-electrolyte; PYE: PY-electrolyte.

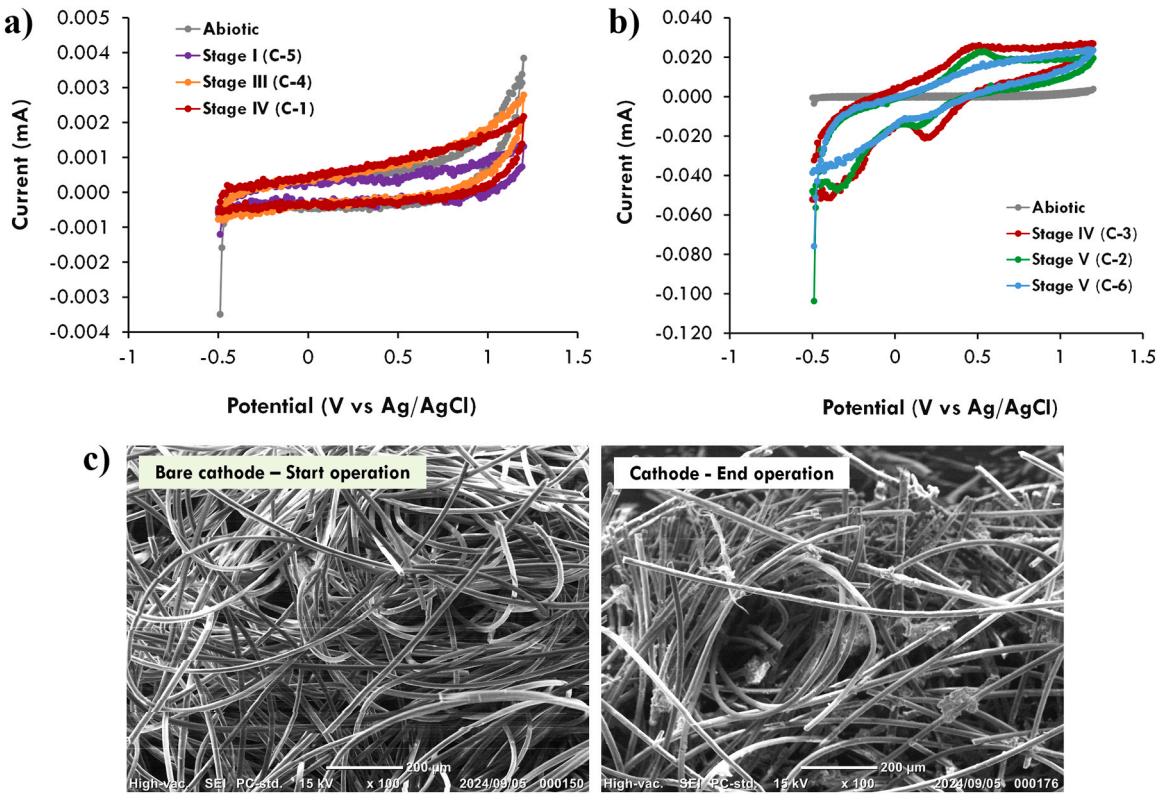

Fig. 3. Cyclic voltammetry of a) high H_2 production b) enhanced CH_4 generation, and c) biofilm formation.

the prevalence of EAB [48]. The fluctuations observed in the CV curves might have resulted from biological variations and non-uniform biofilm distribution on the electrode surface rather than from electrochemical instability. The overall redox profile showed consistent trends across replicates. SEM analysis also confirmed the biofilm formation on the cathode surface at the end of the reactor operation (Fig. 3c).

3.3. Characteristics of microbial community

3.3.1. Microbial diversity and predominant populations

The microbial community was analyzed in the inoculum and at the end of stage III-cycle 4 (EME-0.7 V), stage IV-cycle 4 (PYE-0.35 V), and stage V-cycle 6 (PYE-0.15 V). The rarefaction curves of ASVs for the samples reached a plateau (Fig. S2) with the Good's coverage values ranging from 0.98 to 1.00, indicating sufficient sequencing depth to capture the observed microbial diversity. Furthermore, the alpha diversity of microbial communities estimated by the Shannon and Simpson indices was lower for the reactor samples than for the inoculum and tended to be higher when PYE was used than when EYE was used (Table S2).

In all the samples analyzed, bacteria accounted for at least 92.5 % of the total microbial community. The phyla Bacteroidota, Campylobacterota, Desulfobacterota, Firmicutes, Proteobacteria, Synergistota and Halobacteriota were predominant, accounting for 57.3–93.7 % of the total community (Fig. S3). Bacteroidota, Firmicutes, and Proteobacteria include typical fermentative bacteria (FEB), exoelectrogens, and hydrogen-producing bacteria (HYD-PB) [49–51]. Among them, Proteobacteria were the most dominant when EYE was used. After changing the electrolyte to PYE, Bacteroidota and Firmicutes became dominant, and Desulfobacterota, Halobacteria, and Synergistota were also increased. Synergistota can degrade small molecules, such as propionic acid and butyric acid, and can interact with methanogens in mutual metabolism [52].

The genera with relative abundances greater than 2 % in at least one sample are summarized in Fig. 4a. *Bacillus* showed higher relative abundance in the cathode biofilm with EME – 0.7 V (5.12 %) than in PYE – 0.15 V (3.17 %). *Bacillus* can exhibit high hydrolytic activities and are regarded as excellent candidates for biological H_2 production [53]. Meanwhile, the operation with PYE-0.15 V led to the increased relative abundance of *Desulfovibrio,* which was categorized as syntrophic bacteria (SYB), and *Geobacter* at the cathode biofilms from 0.12 % to 4.00 % and from 0.31 % to 0.74 %, respectively. *Geobacter* is well-known to donate electrons to methanogens via a DIET pathway [54,55]. The abundance of *Petrimonas* was also increased to 6.2 % under operation with PYE - 0.15 V, respectively. This increase can enhance the conversion of VFAs into acetate which can be utilized by methanogens to generate CH_4 [56]. The syntrophic reactions of *Petrimonas* and *Methanosarcina* have been reported to cause efficient VFAs degradation and CH_4 yield increment [57].

Additionally, the relative abundance of EAB, such as *JGI-0000079-D21* and *DMER64*, at the cathode biofilms increased from 0.2 % and 0 % at EME-0.7 V to 3.6 % and 4.4 % at PYE-0.15 V, respectively. This increase promoted the degradation of sCOD and VFAs, followed by an increase of CH_4 generation. *JGI-0000079-D21* was reported as EAB with an extracellular electron transfer (EET) potential in electrochemical system [58]. Meanwhile, the enrichment of *DMER64* was reported to promote methanogen growth, which potentially accelerates CH_4 production and facilitates the DIET pathway [59].

Within the archaeal communities, the dominant methanogens at cathode biofilms were shifted from *Methanosaeta* at EME-0.7 V (70 %) to *Methanosarcina* and *Methanoculleus* at PYE-0.15 V (57.9 % and 36.2 %, respectively). *Methanosaeta* is a typical acetoclastic methanogens (ACEMETs), whereas *Methanosarcina* is a versatile methanogen that can utilize a variety of substrates, such as acetate, methanol, and hydrogen for methanogenesis [60]. *Methanosarcina* is also known as a cytochrome-containing methanogen that can engage in the direct EET and DIET pathways within syntrophic communities [61,62], and is involved in EM through directly acquiring extracellular electrons from

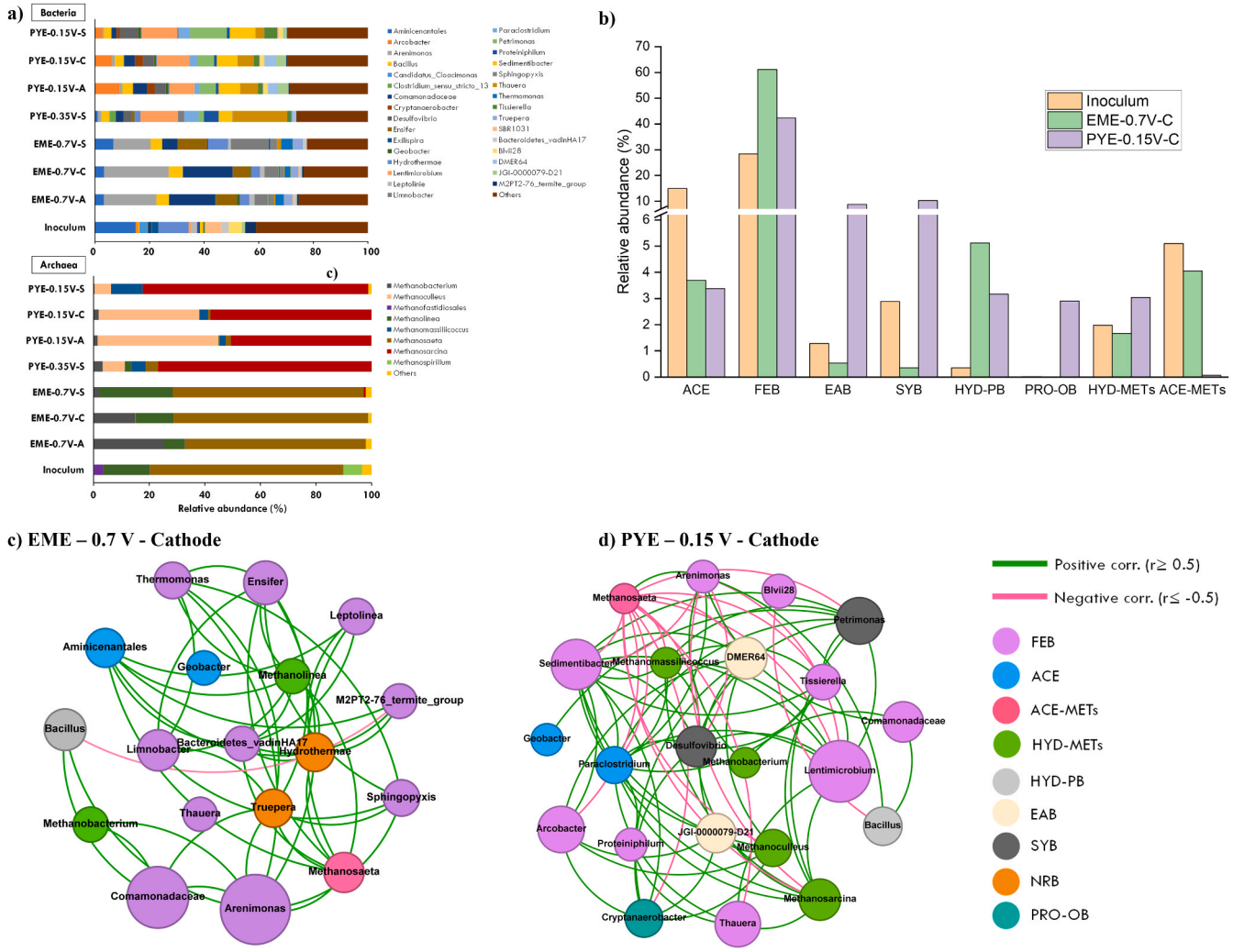

Fig. 4. a) Microbial composition at genus level (relative abundance (>2 %), b) distribution of functional genera, and visualization of microbial ecological network of: c) EME-0.7 V - Cathode and d) PYE-0.15 V - Cathode (the size of nodes represents relative abundance of genera and proportional to the number of connections). C: Cathode; A: Anode; S: suspended sludge; FEB: fermentative bacteria; ACE: acetogen; ACE-METs: acetoclastic methanogens; HYD-METs: hydrogenotrophic methanogens; HYD-PB: hydrogen-producing bacteria; EAB: electroactive bacteria; SYB: syntrophic bacteria; NRB: nitrogen-reducing bacteria; PRO-OB: propionate oxidizing bacteria.

electrodes [63]. The pathways of methanogenesis and interspecies H_2 transfer (IHT) were strongly enhanced by *DMER64* and *Methanosarcina* as the main H_2 carrier and dominant methanogens, respectively [64,65].

A KEGG-based metabolic pathway prediction was performed to identify key enzymes potentially involved in the EM system and to elucidate the metabolic mechanisms underlying the enhanced EM performance (Fig. S4a). The analysis revealed that the key enzymes involved in mediated interspecies electron transfer (MIET) (formate dehydrogenase, EC:1.2.1.2; hydrogenase, EC:1.12.1.3) were relatively higher in PYE-0.15 V than in EME, supporting the promotion of interspecies electron transfer via hydrogen/formate (Fig. S4b). Meanwhile, DIET-associated enzymes (cytochrome-c oxidase, EC:7.1.1.9; riboflavin kinase/synthase, EC:2.5.1.9, EC:2.7.7.2, and EC:2.7.1.26) were also enriched in PYE, suggesting enhanced electron shuttles and DIET through redox-active cofactors.

The enzymes associated with hydrogenotrophic methanogenesis pathway (EC:1.2.99.5, EC:2.1.1.86, EC:2.8.4.1, and EC:1.8.98.1) were also abundant under the PYE-0.15 V condition, indicating a metabolic preference of increased CH_4 production via CO_2 reduction by H_2. These findings support the proposed mechanism in which syntrophic and electroactive microorganisms synergistically contribute to efficient electron transfer and CH_4 generation in the EM system. The KEGG-based metabolic prediction confirms the involvement of these key enzymes in promoting EM process and provides evidence supporting both MIET and DIET-driven methanogenic pathways under the PYE-0.15 V condition.

3.3.2. *Distribution of functional genera*

The genera listed in Fig. 4a were categorized based on their potential functions, and the total abundance of each functional group in the inoculum and cathode biofilms is shown in Fig. 4b. The abundance of FEB and HYD-PB was decreased from 61.1 % and 5.1 % in EME-0.7 V to 42.4 % and 3.2 % in PYE - 0.15 V, respectively. In contrast, the operation in PYE-0.15 V enhanced the abundance of EAB, SYB, PRO-OB, hydrogenotrophic methanogens (HYD-METs), and ACE-METs to 8.7 %, 10.3 %, 2.9 %, 3.0 %, and 4.3 %, respectively. These results indicate that the combination of PYE as an electrolyte and low-voltage can suppress the development of FEB and HYD-PB and stimulate EAB. Recent studies have reported that the application of low-voltage EAB and SYB are interconnected with other microorganisms as core populations [66], and the metabolic activities of EAB are stimulated, which leads to the increased production of electron transfer mediators (e.g., c-type cytochromes, cysteines, and flavins) and consequently more efficient transfer of electrons to electrodes [67]. Additionally. the use of PYE, which is rich in organic carbon, might promote the growth of

methanogens and PRO-OB. HYD-METs can effectively use electrons in the cathode that provided by the EAB, which increases their competitive edge for generating CH_4 [68].

3.3.3. Microbial co-occurrence network

The microbial co-occurrence network analysis revealed that the interactions between microbes in the cathode biofilm varied drastically with the changing operating conditions (Fig. 4b-c). Within the network formed in EME-0.7 V, *Bacillus*, a HYD-PB, showed significant positive interactions with six types of FEB, whereas EAB and SYB were not present (Fig. 4b). *Bacillus* also had a significant negative interaction with *M2PT2–76_termite_group* as FEB, suggesting their competition for the same substrates/nutrients.

Meanwhile, in PYE-0.15 V, two types of EAB and SYB in addition to four types of HYD-METs and one type of ACE-METs showed significant positive correlations (Fig. 4c). Thus, the use of PYE with at a low-voltage likely promotes symbiotic interactions and collaboration with HYD-METs in generating CH_4. Especially, *Geobacter* exhibited a positive linkage with both of *Petrimonas* (as SYB) and HYD-METs. This indicated that *Geobacter* promotes CH_4 generation by enabling positive syntrophic associations with HYD-METs. *Geobacter* can produce several redox-active proteins and form nanowire networks in its extracellular matrix, which mediates EET to the syntrophic companions [69]. The syntrophic mechanism between SYB and HYD-METs is another essential process for higher CH_4 generation.

In contrast to HYD-METs, *Methanosaeta* showed negative interactions with 12 genera in the PYE–0.15 V. This might be caused by the negative response of *Methanosaeta* to the high acetate concentration when PYE was applied, owing to their higher affinity to acetate and suppressed dominance under high acetate levels [70]. In addition, one type of PRO-OB exhibited positive associations with multiple functional bacteria with the EET potential, including SYB, FEB, and EAB. Enhanced CH_4 generation with PYE and a low applied voltage might be primarily impacted by dominant positive interactions in the microbial ecological network.

3.4. Correlations between operating conditions, reactor performance, and functional microorganisms

The RDA and Pearson correlation analyses were performed to identify correlations between operating conditions, reactor performance, and functional microorganisms. Similar results were obtained in both analyses (Fig. 5; Fig. S5). Notably, SYB demonstrated significant responsiveness with PYE and applied voltage of 0.15 V, which revealed a positive association with CH_4 generation, whereas the operation with EME at 0.7 V showed strong correlation with H_2 generation.

In the Pearson correlation analysis, the use of EME as an electrolyte showed a positive correlation with H_2 generation ($r = 0.97$), whereas the use of PYE was positively correlated with CH_4 production ($r = 0.94$). Meanwhile, a low applied voltage was positively correlated with the abundance of SYB ($r = 0.91$), which had a positive correlation with CH_4 production ($r = 0.93$). Applying a low-voltage of 0.15 V showed a higher correlation ($r = 0.79$) with the increasing abundance of EAB. There were also positive correlations between EAB and HYD-METs

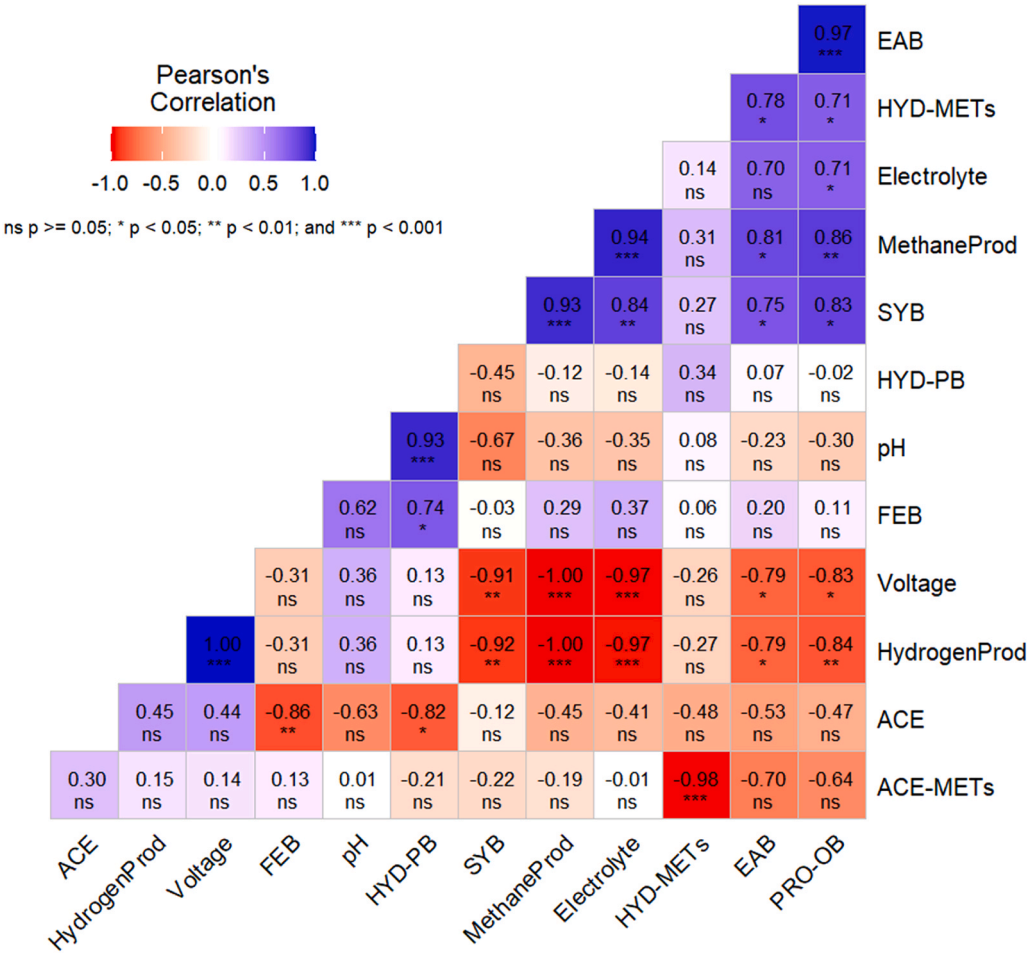

Fig. 5. Correlation analysis between different electrolyte compositions and applied voltages to environmental conditions, and functional microbial communities. ACE: acetogens; ACE-METs: acetoclastic methanogens; EAB: electroactive bacteria; FEB: fermentative bacteria; HYD-METs: hydrogenotrophic methanogens; HYD-PB: hydrogen-producing bacteria; PRO-OB: propionate-oxidizing bacteria; SYB: syntrophic bacteria.

(r = 0.78), EAB and SYB (r = 0.75), and SYB and HYD-METs (r = 0.27), suggesting their cooperative associations for enhanced CH_4 generation. Furthermore, the abundance of PRO-OB was positively correlated with SYB (r = 0.83), EAB (r = 0.97), HYD-METs (r = 0.71), and CH_4 productivity (r = 0.86). Collectively, these results indicate that enhanced CH_4 production in the EM system was achieved through the complex collaborative interactions of multiple functional groups, including EAB, SYB, PRO-OB, and HYD-METs, which were supported by organic-rich conditions and a lower applied voltage.

4. Conclusions

The findings of this study indicated the use of PYE at a low applied voltage of 0.15 V offers great potential for the establishment of EM system. An organic-rich electrolyte revealed the significance of the substrate composition in shaping the electrode biofilm; hence, it is essential to carefully select the electrolyte composition for the successful start-up of the EM system. Meanwhile, a low applied voltage (0.15 V) promoted electrochemically active microbial activity in the EM system, which was beneficial for promoting CH_4 generation. *Methanosarcina* (57.9 %) and *Methanoculleus* (36.2 %) dominated at the biocathode archaeal community with PYE at applied voltage 0.15 V. SYB and EAB also exist and are putatively involved in the electron transfer for CH_4 generation that facilitated by the DIET pathway. These findings highlight the critical role of microbial community dynamics in promoting CH_4 generation and imply that the development of reliable renewable energy storage systems can be aided by the operation of EM with low-voltage and organic-rich electrolyte composition.

CRediT authorship contribution statement

Lucky Caesar Direstiyani: Writing – original draft, Visualization, Methodology, Investigation, Formal analysis, Data curation, Conceptualization. **Michihiko Ike:** Writing – review & editing, Supervision, Resources, Conceptualization. **Daisuke Inoue:** Writing – review & editing, Visualization, Supervision, Resources, Conceptualization.

Funding sources

This study did not receive any specific grant from funding agencies in the public, commercial, or not-for-profit sectors.

Declaration of Competing Interest

The authors declare that they have no known competing financial interests or personal relationships that could have appeared to influence the work reported in this paper.

Acknowledgements

Lucky Caesar Direstiyani gratefully acknowledges the financial support provided by Japan International Cooperation Agency (JICA) during doctoral study. We would like to thank Ms. Tomoka Yokoi and Dr. Ryusei Ito from Takuma Co., Ltd., Japan, for constructive discussions and valuable suggestions during this study. Grateful acknowledgment is extended to Prof. Masahiro Takeo and Dr. Hidehiro Ishizawa from University of Hyogo for the generous support and assistance for the SEM analysis. We would also thank Editage (www.editage.com) for the English language editing.

Appendix A. Supporting information

Supplementary data associated with this article can be found in the online version at doi:10.1016/j.bej.2025.110035.

Data availability

Data will be made available on request.

References

[1] A. Castillo, D.F. Gayme, Grid-scale energy storage applications in renewable energy integration: a survey, Energy Convers. Manag 87 (2014) 885–894, https://doi.org/10.1016/j.enconman.2014.07.063.
[2] H. Blanco, W. Nijs, J. Ruf, A. Faaij, Potential of Power-to-Methane in the EU energy transition to a low carbon system using cost optimization, Appl. Energy 232 (2018) 323–340, https://doi.org/10.1016/j.apenergy.2018.08.027.
[3] M.A. Mirzaei, M. Habibi, V. Vahidinasab, B. Mohammadi-Ivatloo, Concept, environmental benefits and working mechanism of power-to-gas (P2G) technology, Elsevier eBooks, 2023, pp. 29–46, https://doi.org/10.1016/b978-0-323-90544-2.00001-4.
[4] S. Cheng, D. Xing, D.F. Call, B.E. Logan, Direct biological conversion of electrical current into methane by electromethanogenesis, Environ. Sci. Technol. 43 (2009) 3953–3958, https://doi.org/10.1021/es803531g.
[5] A. Ceballos-Escalera, D. Molognoni, P. Bosch-Jimenez, M. Shahparasti, S. Bouchakour, A. Luna, A. Guisasola, E. Borràs, M. Della Pirriera, Bioelectrochemical systems for energy storage: a scaled-up power-to-gas approach, Appl. Energy 260 (2019) 114138, https://doi.org/10.1016/j.apenergy.2019.114138.
[6] N. Aryal, L.D.M. Ottosen, M.V.W. Kofoed, D. Pant, Emerging technologies and biological systems for biogas upgrading (1ed), Academic Press, 2021, https://doi.org/10.1016/C2019-0-01200-9.
[7] G. Buitrón, R. Cardeña, J.S. Arcila, Bioelectrosynthesis of methane integrated with anaerobic digestion, Elsevier eBooks, 2019, pp. 899–919, https://doi.org/10.1016/b978-0-444-64052-9.00037-6.
[8] A. Ding, Y. Yang, G. Sun, D. Wu, Impact of applied voltage on methane generation and microbial activities in an anaerobic microbial electrolysis cell (MEC), Chem. Eng. J. 283 (2016) 260–265, https://doi.org/10.1016/j.cej.2015.07.054.
[9] J. Zhang, Y. Zhang, X. Quan, S. Chen, S. Afzal, Enhanced anaerobic digestion of organic contaminants containing diverse microbial population by combined microbial electrolysis cell (MEC) and anaerobic reactor under Fe(III) reducing conditions, Bioresour. Technol. 136 (2013) 273–280, https://doi.org/10.1016/j.biortech.2013.02.103.
[10] W. Liu, Y. Piao, F. Zhang, L. Liu, D. Meng, J. Nan, Y. Deng, A. Wang, Hydrogen consumption and methanogenic community evolution in anodophilic biofilms in single chamber microbial electrolysis cells under different startup modes, Environ. Sci. Water Res. Technol. 4 (11) (2018) 1839–1850, https://doi.org/10.1039/c8ew00357b.
[11] H. Zhou, D. Xing, M. Xu, Y. Su, J. Ma, I. Angelidaki, Y. Zhang, Optimization of a newly developed electromethanogenesis for the highest record of methane production, J. Hazard. Mater. 407 (2021) 124363, https://doi.org/10.1016/j.jhazmat.2020.124363.
[12] Z. Dou, C.M. Dykstra, S.G. Pavlostathis, Bioelectrochemically assisted anaerobic digestion system for biogas upgrading and enhanced methane production, Sci. Total Environ. 633 (2018) 1012–1021, https://doi.org/10.1016/j.scitotenv.2018.03.255.
[13] K. Verbeeck, J. De Vrieze, M. Biesemans, K. Rabaey, Membrane electrolysis-assisted CO_2 and H_2S extraction as innovative pretreatment method for biological biogas upgrading, Chem. Eng. J. 361 (2019) 1479–1486, https://doi.org/10.1016/j.cej.2018.09.120.
[14] R. Blasco-Gomez, P. Batlle-Vilanova, M. Villano, M.D. Balaguer, J. Colprim, S. Puig, On the edge of research and technological application: a critical review of electromethanogenesis, Int. J. Mol. Sci. 18 (2017) 1–32, https://doi.org/10.3390/ijms18040874.
[15] W. Cai, W. Liu, Z. Zhang, K. Feng, G. Ren, C. Pu, H. Sun, J. Li, Y. Deng, A. Wang, mcrA sequencing reveals the role of basophilic methanogens in a cathodic methanogenic community, Water Res. 136 (2018) 192–199, https://doi.org/10.1016/j.watres.2018.02.062.
[16] L. Luo, S. Xu, Y. Jin, R. Han, H. Liu, F. Lü, Evaluation of methanogenic microbial electrolysis cells under closed/open circuit operations, Environ. Technol. 39 (6) (2018) 739–748, https://doi.org/10.1080/09593330.2017.1310934.
[17] N. LaBarge, Y.D. Yilmazel, P. Hong, B.E. Logan, Effect of pre-acclimation of granular activated carbon on microbial electrolysis cell startup and performance, Bioelectrochemistry 113 (2017) 20–25, https://doi.org/10.1016/j.bioelechem.2016.08.003.
[18] A.A. Pawar, A. Karthic, S. Lee, S. Pandit, S.P. Jung, Microbial electrolysis cells for electromethanogenesis: materials, configurations and operations, Environ. Eng. Res. 27 (1) (2022), https://doi.org/10.4491/eer.2020.484, 200484-0.
[19] R.M. Alonso, A. Escapa, A. Sotres, A. Morán, Integrating microbial electrochemical technologies with anaerobic digestion to accelerate propionate degradation, Fuel 267 (2020) 117158, https://doi.org/10.1016/j.fuel.2020.117158.
[20] D. Carrillo-Peña, R. Mateos, A. Morán, A. Escapa, Reduced graphene oxide improves the performance of a methanogenic biocathode, Fuel 321 (2022) 123957, https://doi.org/10.1016/j.fuel.2022.123957.
[21] G. Pelaz, J. González-Arias, R. Mateos, A. Escapa, Electromethanogenesis for the conversion of hydrothermal carbonization exhaust gases into methane, Renew. Energy 216 (2023) 119047, https://doi.org/10.1016/j.renene.2023.119047.

[22] A. Ghaderikia, B. Taskin, Y.D. Yilmazel, Start-up strategies of electromethanogenic reactors for methane production from cattle manure, Waste Manag 159 (2023) 27–38, https://doi.org/10.1016/j.wasman.2023.01.027.
[23] K. Dalkılıç, K, E. Aghayev, E. Sinoplu, E, Voltage application and biomass retention increased biogas production in a combined microbial electrolysis cell and anaerobic digestion system treating chicken manure, Biochem. Eng. J. 219 (2025) 109728, https://doi.org/10.1016/j.bej.2025.109728.
[24] Q. Feng, Y. Song, Surface modification of a graphite fiber fabric anode for enhanced bioelectrochemical methane production, Energy Fuels 30 (8) (2016) 6467–6474, https://doi.org/10.1021/acs.energyfuels.6b00959.
[25] Z. Zhao, Y. Zhang, W. Ma, J. Sun, S. Sun, X. Quan, Enriching functional microbes with electrode to accelerate the decomposition of complex substrates during anaerobic digestion of municipal sludge, Biochem. Eng. J. 111 (2016) 1–9, https://doi.org/10.1016/j.bej.2016.03.002.
[26] S. Colantoni, D. Molognoni, P. Sánchez-Cueto, C. De Soto, P. Bosch-Jimenez, R. Ghemis, E. Borràs, Bioelectrochemically-improved anaerobic digestion of fishery processing industrial wastewater, J. Water Process Eng. 65 (2024) 105848, https://doi.org/10.1016/j.jwpe.2024.105848.
[27] M.C.A.A. Van Eerten-Jansen, A.B. Veldhoen, C.M. Plugge, A.J.M. Stams, C.J. N. Buisman, A.T. Heijne, Microbial community analysis of a methane-producing biocathode in a bioelectrochemical system, Archaea 2013 (2013) 481784, https://doi.org/10.1155/2013/481784.
[28] C.W. Marshall, D.E. Ross, E.B. Fichot, R.S. Norman, H.D. May, Electrosynthesis of commodity chemicals by an autotrophic microbial community, Appl. Environ. Microb. 78 (23) (2012) 8412–8420, https://doi.org/10.1128/aem.02401-12.
[29] APHA. Standard Method for Examination of Water and Wastewater, 22nd ed., American Public Health Association, Washington, DC, USA, 2012.
[30] G. Peixoto, J.L.R. Pantoja-Filho, J.A.B. Agnelli, M. Barboza, M. Zaiat, Hydrogen and methane production, energy recovery, and organic matter removal from effluents in a two-stage fermentative process, Appl. Biochem. Biotechnol. 168 (3) (2012) 651–671, https://doi.org/10.1007/s12010-012-9807-4.
[31] A. Kas, Y.D. Yilmazel, High current density via direct electron transfer by hyperthermophilic archaeon, *Geoglobus acetivorans*, in microbial electrolysis cells operated at 80∘C, Bioelectrochemistry 145 (2022) 108072, https://doi.org/10.1016/j.bioelechem.2022.108072.
[32] N. Isozumi, Y. Masubuchi, T. Imamura, M. Mori, H. Koga, S. Ohki, Structure and antimicrobial activity of NCR169, a nodule-specific cysteine-rich peptide of *Medicago truncatula*. Sci. Rep. 11 (2021) 9923, https://doi.org/10.1038/s41598-021-89485-w.
[33] J.G. Caporaso, C.L. Lauber, W.A. Walters, D. Berg-Lyons, C.A. Lozupone, P. J. Turnbaugh, N. Fierer, R. Knight, Global patterns of 16S rRNA diversity at a depth of millions of sequences per sample, Proc. Natl. Acad. Sci. 108 (2011) 4516–4522, https://doi.org/10.1073/pnas.1000080107.
[34] J.A. Peiffer, A. Spor, O. Koren, Z. Jin, S.G. Tringe, J.L. Dangl, E.S. Buckler, R.E. Ley, Diversity and heritability of the maize rhizosphere microbiome under field conditions, Proc. Natl. Acad. Sci. 110 (2013) 6548–6553, https://doi.org/10.1073/pnas.1302837110.
[35] G.M. Douglas, V.J. Maffei, J.R. Zaneveld, S.N. Yurgel, J.R. Brown, C.M. Taylor, C. Huttenhower, M.G.I. Langille, PICRUSt2 for prediction of metagenome functions, Nat. Biotechnol. 38 (6) (2020) 685–688, https://doi.org/10.1038/s41587-020-0548-6.
[36] M. Bastian, S. Heymann, M. Jacomy, Gephi: an open source software for exploring and manipulating networks, in: Proceedings of the International AAAI Conference on Web and Social Media, 3, 2009, pp. 361–362, https://doi.org/10.1609/icwsm.v3i1.13937.
[37] A.W. Jeremiasse, H.V. Hamelers, C.J. Buisman, Microbial electrolysis cell with a microbial biocathode, Bioelectrochemistry 78 (1) (2009) 39–43, https://doi.org/10.1016/j.bioelechem.2009.05.005.
[38] S. Georg, I. De Eguren Cordoba, T. Sleutels, P. Kuntke, A.Ter Heijne, C. Buisman, Competition of electrogens with methanogens for hydrogen in bioanodes, Water Res. 170 (2020) 115292, https://doi.org/10.1016/j.watres.2019.115292.
[39] G. Pelaz, D. Carrillo-Peña, A. Morán, A. Escapa, Electromethanogenesis at medium-low temperatures: Impact on performance and sources of variability, Fuel 310 (2022) 122336, https://doi.org/10.1016/j.fuel.2021.122336.
[40] X. Hao, Q. Wang, J. Zhu, M.C.M. Van Loosdrecht, Microbiological endogenous processes in biological wastewater treatment systems, Crit. Rev. Environ. Sci. Technol. 40 (3) (2010) 239–265, https://doi.org/10.1080/10643380802278901.
[41] Q. Wang, K. Song, X. Hao, J. Wei, M. Pijuan, M.C.M. Van Loosdrecht, H. Zhao, Evaluating death and activity decay of Anammox bacteria during anaerobic and aerobic starvation, Chemosphere 201 (2018) 25–31, https://doi.org/10.1016/j.chemosphere.2018.02.171.
[42] F. Ndayisenga, Z. Yu, B. Wang, D. Zhou, Effects of the applied voltage on electroactive microbial biofilm viability and hydrogen production in a recalcitrant organic waste-fed single-chamber membrane-free microbial electrolysis cell performance, Chem. Eng. J. 469 (2023) 144002, https://doi.org/10.1016/j.cej.2023.144002.
[43] M. Masuda, S. Freguia, Y.F. Wang, S. Tsujimura, K. Kano, Flavins contained in yeast extract are exploited for anodic electron transfer by *Lactococcus lactis*, Bioelectrochemistry 78 (2) (2010) 173–175, https://doi.org/10.1016/j.bioelechem.2009.08.004.
[44] K. Fenn, P. Strandwitz, E.J. Stewart, E. Dimise, S. Rubin, S. Gurubacharya, J. Clardy, K. Lewis, Quinones are growth factors for the human gut microbiota, Microbiome 5 (1) (2017) 161, https://doi.org/10.1186/s40168-017-0380-5.
[45] M. Villano, F. Aulenta, C. Ciucci, T. Ferri, A. Giuliano, M. Majone, Bioelectrochemical reduction of CO_2 to CH_4 via direct and indirect extracellular electron transfer by a hydrogenophilic methanogenic culture, Bioresour. Technol. 101 (9) (2010) 3085–3090, https://doi.org/10.1016/j.biortech.2009.12.077.
[46] F.M. Silva, C.F. Mahler, L.B. Oliveira, J.P. Bassin, Hydrogen and methane production in a two-stage anaerobic digestion system by co-digestion of food waste, sewage sludge and glycerol, Waste Manag. 76 (2018) 339–349, https://doi.org/10.1016/j.wasman.2018.02.039.
[47] K. Fricke, F. Harnisch, U. Schröder, On the use of cyclic voltammetry for the study of anodic electron transfer in microbial fuel cells, Energy Environ. Sci. 1 (1) (2008) 144, https://doi.org/10.1039/b802363h.
[48] A. Escapa, R. Mateos, E. Martínez, J. Blanes, Microbial electrolysis cells: an emerging technology for wastewater treatment and energy recovery. From laboratory to pilot plant and beyond, Renew. Sustain. Energy Rev. 55 (2015) 942–956, https://doi.org/10.1016/j.rser.2015.11.029.
[49] Z. Liu, A. Zhou, H. Liu, S. Wang, W. Liu, A. Wang, X. Yue, Extracellular polymeric substance decomposition linked to hydrogen recovery from waste activated sludge: Role of peracetic acid and free nitrous acid co-pretreatment in a prefermentation-bioelectrolysis cascading system, Water Res. 176 (2020) 115724, https://doi.org/10.1016/j.watres.2020.115724.
[50] Q. Gao, Q. Zhao, K. Wang, X. Li, H. Zhou, J. Ding, L. Li, Promoting methane production during anaerobic digestion with biochar: is it influenced by quorum sensing? Chem. Eng. J. 483 (2024) 149268 https://doi.org/10.1016/j.cej.2024.149268.
[51] Y. Ichikawa, H. Yamamoto, S. Hirano, B. Sato, Y. Takefuji, F. Satoh, The overlooked benefits of hydrogen-producing bacteria, Med. Gas. Res. 13 (3) (2022) 108–111, https://doi.org/10.4103/2045-9912.344977.
[52] R. Han, D. Zhu, J. Xing, Q. Li, Y. Li, L. Chen, The effect of temperature fluctuation on the microbial diversity and community structure of rural household biogas digesters at Qinghai Plateau, Arch. Microbiol. 202 (3) (2020) 525–538, https://doi.org/10.1007/s00203-019-01767-0.
[53] A. Shah, L. Favaro, L. Alibardi, L. Cagnin, A. Sandon, R. Cossu, S. Casella, M. Basaglia, *Bacillus* sp. strains to produce bio-hydrogen from the organic fraction of municipal solid waste, Appl. Energy 176 (2016) 116–124, https://doi.org/10.1016/j.apenergy.2016.05.054.
[54] L. Wang, K.P. Nevin, T.L. Woodard, B. Mu, D.R. Lovley, Expanding the diet for DIET: Electron donors supporting direct interspecies electron transfer (DIET) in defined Co-Cultures, Front. Microbiol. 7 (2016) 236, https://doi.org/10.3389/fmicb.2016.00236.
[55] S. Zheng, M. Li, Y. Liu, F. Liu, Desulfovibrio feeding Methanobacterium with electrons in conductive methanogenic aggregates from coastal zones, Water Res. 202 (2021) 117490, https://doi.org/10.1016/j.watres.2021.117490.
[56] R. Wang, J. Gu, Q. Wang, S. Jiang, Z. Wu, J. Wang, G. Li, X. Gong, Enhancing methane production in dry anaerobic digestion of ruminant manures through substrates ratio regulation for strengthened microbial interactions, Environ. Technol. Innov. 32 (2023) 103389, https://doi.org/10.1016/j.eti.2023.103389.
[57] G. Wang, Q. Li, Y. Li, Y. Xing, G. Yao, Y. Liu, R. Chen, X.C. Wang, Redox-active biochar facilitates potential electron transfer between syntrophic partners to enhance anaerobic digestion under high organic loading rate, Bioresour. Technol. 298 (2019) 122524, https://doi.org/10.1016/j.biortech.2019.122524.
[58] X. Qi, X. Jia, Y. Wang, P. Xu, M. Li, B. Xi, Y. Zhao, Y. Zhu, F. Meng, M. Ye, Development of a rapid startup method of direct electron transfer-dominant methanogenic microbial electrosynthesis, Bioresour. Technol. 358 (2022) 127385, https://doi.org/10.1016/j.biortech.2022.127385.
[59] Y. Hu, X. Wang, S. Zhang, S. Liu, T. Hu, X. Wang, C. Wang, J. Wu, L. Xu, G. Xu, F. Hu, Microbial response behavior to powdered activated carbon in high-solids anaerobic digestion of kitchen waste: metabolism and functional prediction analysis, J. Environ. Manag. 337 (2023) 117756, https://doi.org/10.1016/j.jenvman.2023.117756.
[60] D. Batstone, T. Hülsen, A. Oehmen, Metabolic modelling of mixed culture anaerobic microbial processes, Curr. Opin. Biotechnol. 57 (2019) 137–144, https://doi.org/10.1016/j.copbio.2019.03.014.
[61] A.R. Rowe, S. Xu, E. Gardel, A. Bose, P. Girguis, J.P. Amend, M.Y. El-Naggar, Methane-linked mechanisms of electron uptake from cathodes by *Methanosarcina barkeri*, mBio 10 (2019) e02448–18, https://doi.org/10.1128/mbio.02448-18.
[62] D.E. Holmes, J. Zhou, T. Ueki, T. Woodard, D.R. Lovley, Mechanisms for electron uptake by *Methanosarcina acetivorans* during direct interspecies electron transfer, mBio 12 (2021) e02344–21, https://doi.org/10.1128/mbio.02344-21.
[63] M.O. Yee, O.L. Snoeyenbos-West, B. Thamdrup, L.D.M. Ottosen, A. Rotaru, Extracellular electron uptake by two *Methanosarcina* species, Front. Energy Res. 7 (2019) 29, https://doi.org/10.3389/fenrg.2019.00029.
[64] X. Meng, Q. Cao, Y. Sun, S. Huang, X. Liu, D. Li, 16S rRNA genes- and metagenome-based confirmation of syntrophic butyrate-oxidizing methanogenesis enriched in high butyrate loading, Bioresour. Technol. 345 (2021) 126483, https://doi.org/10.1016/j.biortech.2021.126483.
[65] H. Zhuang, G.A. Tan, H. Jing, P. Lee, D. Lee, S. Leu, Enhanced primary treatment for net energy production from sewage – The genetic clarification of substrate-acetate-methane pathway in anaerobic digestion, Chem. Eng. J. 431 (2021) 133416, https://doi.org/10.1016/j.cej.2021.133416.
[66] X. Wang, L. Zhao, Q. Zhang, B. Wang, D. Xing, J. Nan, N. Ren, D. Lee, C. Chen, Linking performance to dynamic migration of biofilm ecosystem reveals the role of voltage in the start-up of hybrid microbial electrolysis cell-anaerobic digestion, Bioresour. Technol. 411 (2024) 131242, https://doi.org/10.1016/j.biortech.2024.131242.
[67] H. Huang, Y. Yang, S. Yang, X. Yang, Y. Huang, M. Dong, S. Zhou, M. Xu, Filamentous electroactive microorganisms promote mass transfer and sulfate reduction in sediment microbial electrochemical systems, Chem. Eng. J. 466 (2023) 143214, https://doi.org/10.1016/j.cej.2023.143214.

[68] X. Wang, L. Zhao, C. Chen, K. Chen, H. Yang, X. Xu, X. Zhou, W. Liu, D. Xing, N. Ren, D. Lee, Microbial electrolysis cells (MEC) accelerated methane production from the enhanced hydrolysis and acidogenesis of raw waste activated sludge, Chem. Eng. J. 413 (2021) 127472, https://doi.org/10.1016/j.cej.2020.127472.
[69] G. Yang, L. Huang, Z. Yu, X. Liu, S. Chen, J. Zeng, S. Zhou, L. Zhuang, Anode potentials regulate *Geobacter* biofilms: New insights from the composition and spatial structure of extracellular polymeric substances, Water Res. 159 (2019) 294–301, https://doi.org/10.1016/j.watres.2019.05.027.
[70] K.S. Smith, C. Ingram-Smith, *Methanosaeta*, the forgotten methanogen? Trends Microbiol. 15 (4) (2007) 150–155, https://doi.org/10.1016/j.tim.2007.02.002.